MODELING WAITING BEHAVIOR AT TRAIN STATIONS WITH CELLULAR AUTOMATON

Tobias Schrödter¹ and Mohcine Chraibi¹

¹Institute of Advanced Simulation (IAS-7)
Forschungszentrum Jülich GmbH, 52425 Jülich, Germany
email: t.schroedter@fz-juelich.de, m.chraibi@fz-juelich.de

ABSTRACT

The distribution of passengers waiting on train platforms influences the boarding and alighting times of trains, hence it is one of the limiting factors of the performance of train stations. We introduce a cellular automaton for modeling the pedestrians' waiting behavior at platforms. Different factors as the geometry and the positions of other waiting pedestrians are taken into account. To assess the model, simulations on a excerpt of a real life platform in Bern, Switzerland were performed. The results show good agreement with the observations of previously conducted field studies.

INTRODUCTION

One of the bottlenecks influencing railway stations' performance is the distribution of waiting pedestrians on platforms. Firstly, waiting pedestrians who come to a halt or slow down obstruct other pedestrians in their movement. Secondly, the dwell times of trains highly depend on the pedestrians' distribution on the platform. A more uniform distribution leads to faster boarding times, as the train doors will be used more evenly [13, 5].

Simulations are one tool to investigate and analyze the influence of pedestrian's behavior on platforms. Multiple models exist to describe the movement in a simplified way for moving pedestrians, e.g., by different forces acting on the pedestrians or collision avoidance [6, 2, 14]. An important component in these models is the desired movement direction, towards which pedestrians aim. However due to the presence of other pedestrians and obstacles their direction is deflected. In evacuation or boarding and alighting processes, the desired movement is towards a specific physical goal, e.g., the emergency exit, or the train door. Contrary, in waiting processes, the movement is towards an indistinct goal, which mostly may satisfy personal preferences or can be assumed to be randomly chosen.

As already mentioned, the dwell times of trains is an indicator of the performance of railway transport facilities. In [10], data from a camera system at multiple train stations

in Switzerland is used to analyze the pedestrians' movement in more detail. They focus primarily on identifying hot spots of waiting pedestrians, reporting that pedestrians prefer to wait close to immovable objects, e.g., walls, railings around stairs, allowing them to lean against. Qualitative descriptions of the passengers' longitudinal distribution have been given by studies focusing on the dwell times of trains [5, 15, 9, 13]. These studies observed passengers' clustering around entrances and further platform infrastructure as seats, shelters, and vending machines. More experienced travelers also take the train position at the departing station or the position of less crowded coaches into account when choosing a waiting position. However, no further notions of the distribution of the passengers between the tracks were reported.

Recently, the investigation of inflow processes with experiments under laboratory conditions gained more attention. In [11], different hypotheses of the inflow process are compared with experimental data. Experiments focusing on the inflow to a confined were conducted in [4], where a theoretical description of the process is derived. These works emphasized the attractive or repulsive influences of different parts the geometry. Pedestrian tend to prefer positions close to the boundary but try to avoid positions in which they expect more pedestrians to pass.

In [3] and [7], the influence of waiting/standing pedestrians on the flow of passing pedestrians in train stations were investigated with simulations. In these cases, the waiting position was randomly assigned in designated waiting areas, and the waiting pedestrians would not move. An approach to model the passengers' distribution on a metro platform with a cost function approach is discussed in [16]. Different influence factors as he distance to a particular waiting area, density, length of the waiting area are considered in the introduced cost function.

In this paper, we develop a cellular automaton model to describe the movement of waiting pedestrians on a platform. We define waiting pedestrians, as pedestrians who enter a specific region on a platform, until the awaited event is triggered, e.g., the train's arrival.

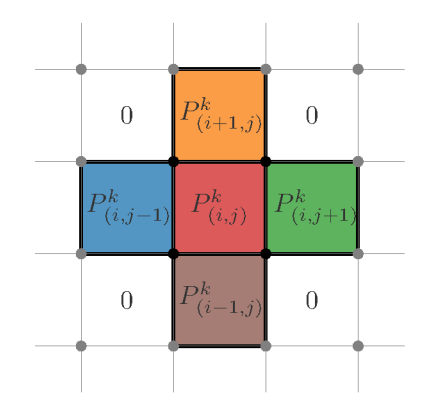
MODEL

The movement of pedestrians in waiting situations depends on the individual's personal preferences. Hence, we propose a heuristic approach based on cellular automata [1, 8]. In this approach, the space is discretized into cells of $0.5 \times 0.5 \, \text{m}^2$, which can be occupied by exactly one person at a time. In each of the compute steps, the pedestrians evaluate their surroundings, deciding for a moving direction. This decision is made by evaluating underlying floor fields representing the potential as waiting position. The higher the potential, the more likely it is that the pedestrian moves in that direction.

A pedestrian k, located in cell (i,j) can move to one of the neighboring cells n of a von Neumann neighborhood N with a given transition probability P_n^k , as in Fig. 1. To determine the probability for each of the neighboring cells multiple floor fields are combined. On one hand, the static floor field S gives an indicator of how preferable a waiting position is, based on influences that will not change during the simulation, for example the distance to walls. On the other hand, the repulsive field R penalizes waiting positions too close to other waiting pedestrians and is updated at each time step, as the pedestrians change their

positions. Additionally, the weight distance field ${\cal W}$ rewards waiting positions close to the current position.

Only the visible area V^k is considered for the computation of the transition probabilities, since pedestrians do not have a global knowledge of the geometry. To identify which cells have an impact on the transition probability of a specific neighbor, the space is divided into Voronoi regions C_n according to the neighbor cells $n \in N$. The visible area and the corresponding Voronoi regions are depicted in Fig. 2, where the union of all colored areas is the visible area. The different colors show which regions impact the probability of a specific neighbor.



5 2 2 -2 -2 -5 -25 -20 -15 -10 -5 0 5

FIGURE 1: Allowed movement direction of pedestrian.

Figure 2: Visibility polygon and the Voronoi regions for the neighboring cells. Colors mark the influence areas of the corresponding neighboring cell from Fig. 1.

As multiple studies report, pedestrians tend to wait close to the platform's entrances. We assume that potential waiting positions close to the current position are preferred to those further away. Hence, with

$$W_{i,j}^{k} = 1 - \left[1 + \exp^{-a_{w} \left(d_{i,j}^{k} - b_{w} \right)} \right]^{-1}, \tag{1}$$

points of interest with a smaller distance d^k to pedestrian k will be rewarded. We use a Sigmoid function to map distances to potentials, with the parameters $a_w, b_w \in \mathbb{R}^+$ controlling the steepness and cut-off radius of a Sigmoid function.

By combining the floor fields, the transition probability of pedestrian k moving to cell $n \in N$ is given by

$$P_n^k = M \cdot \max_{i,j \in V^k \cap C_n} \left(W_{i,j}^k \left[S_{i,j} \cdot R_{i,j}^k \right] \right), \tag{2}$$

where M is a normalization factor such that $\sum_{n\in N} P_n^k = 1$. The floor fields used will be described in detail in the following subsections, together with the algorithm for describing the movement of waiting pedestrians.

Static floor field S

The influences considered in S are the distances to the platform entrances, boundaries, e.g., walls and obstacles, and the platform edge, where the awaited train arrives. These influences do not change over time, as they are only affected by structural features, as fixed walls, door, and obstacles. Pedestrians will try to minimize their distance to regions of interest given by B,T. Moreover, regions close to doors are less preferable as more pedestrians are expected to pass in such regions, this repulsion is represented in E. To model different behavior patterns, the fields are scaled by individual weights $w_b, w_t \in \mathbb{R}^+$. With these assumptions, the potential fields are defined as

$$E_{i,j} = \left[1 + \exp^{-a_e(d_e - b_e)}\right]^{-1},$$
 (3)

$$B_{i,j} = 1 - \left[1 + \exp^{-a_b(d_b - b_b)}\right]^{-1},$$
 (4)

$$T_{i,j} = 1 - \left[1 + \exp^{-a_t(d_t - b_t)}\right]^{-1},$$
 (5)

where d_e, d_b, d_t are the distances to the closest entrance, closest wall, and platform edge, the train will arrive, respectively. The distances are computed with a fast marching approach [12], hence taking detours due to corners or obstacles into account. With the parameters $a_e, b_e, a_b, b_b, a_t, b_t \in \mathbb{R}^+$ the influence area can be controlled.

The resulting static floor field S is defined as

$$S_{i,j} = E_{i,j} \cdot [w_b \cdot B_{i,j} + w_t \cdot T_{i,j}].$$
 (6)

Figs. 3a to 3c show the different potential fields on an excerpt from a platform in Bern, Switzerland. A detailed description of the geometry is given in . Fig. 3d displays the resulting static floor field with Eq. 6.

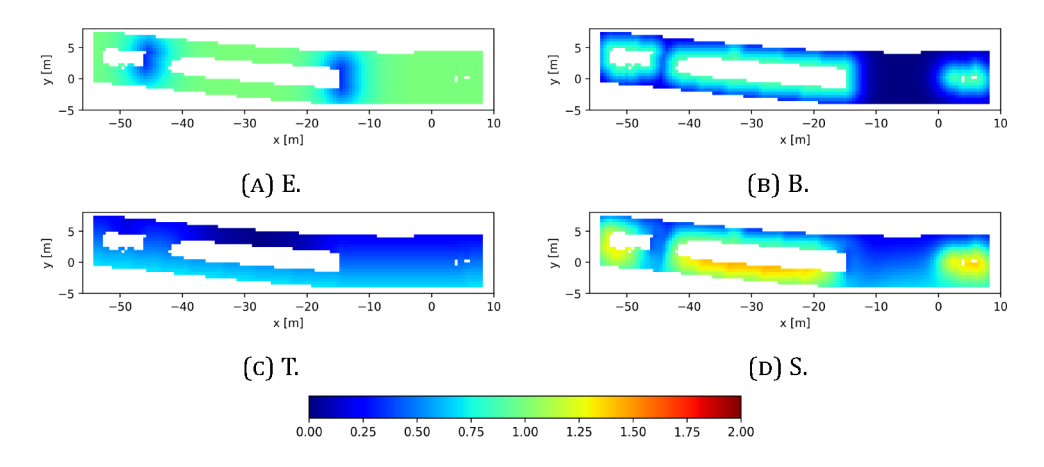


FIGURE 3: Potential of the static influences. More preferable waiting positions are indicated with higher numbers.

Repulsive floor field

As pedestrians prefer waiting positions with a certain distance to other waiting or moving pedestrians the repulsive floor field R is used to penalize areas close to other pedestrians. R is computed in each time step individually for each pedestrian k by

$$R_{i,j}^{k} = \left[1 + \exp^{-a_r \left(d_{i,j}^{k} - b_r\right)}\right]^{-1},\tag{7}$$

where d^k denotes the Euclidean distance to the closest pedestrian. We introduce a cut-off radius to exclude big distances, which can be controlled by $a_r, b_r \in \mathbb{R}^+$. Fig. 4b shows the resulting floor field. Combining all influence factors as in Eq. 2 yields a potential field as in Fig. 4f.

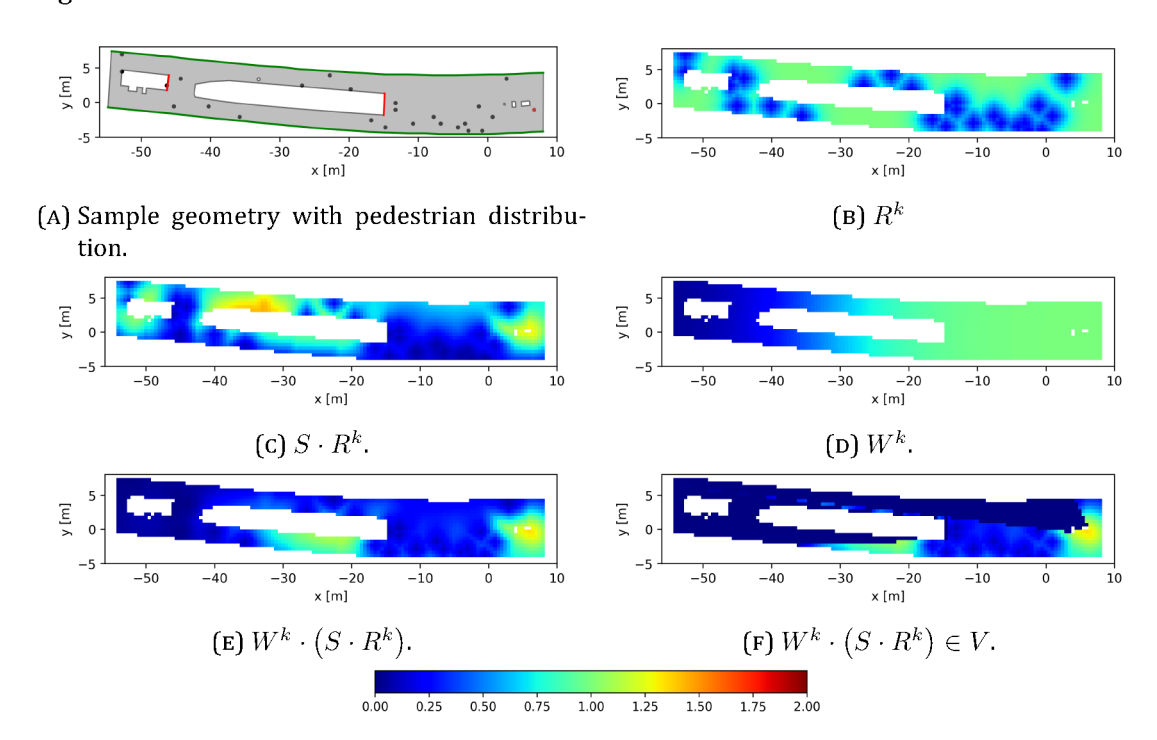


FIGURE 4: The different combinations of floor fields based on the pedestrian distribution on the top. All floor fields are computed for the pedestrian k highlighted in red. A higher number indicates a more preferable waiting position.

Algorithm

The algorithm for determining the pedestrians' movements at a train station is given in 1. It may happen, that multiple pedestrians head towards the same cell, this conflict is solved as described in [1] by using relative probabilities. If one of the pedestrians is already in the target cells, no movement is necessary. Otherwise, one of the pedestrians is chosen randomly based on the relative probabilities. This pedestrian moves towards the target cell, and the others stay at their positions.

Algorithm 1 Simulate waiting pedestrians on platform.

Compute S according to Eq. 6

while maximum of compute steps not reached do

for all pedestrians k on the platform **do**

Compute visible area V^k from current position;

Compute Voronoi regions C of pedestrian and its neighbors;

Compute W^k according to Eq. 1;

Compute R^k according to Eq. 7;

Compute P_n^k according to Eq. 2;

Determine next step based on P;

end for

Solve conflicts;

Move pedestrians according to their next step;

end while

RESULTS

With the model we simulate the waiting behaviors of passengers on an excerpt from a real platform in Bern (track 3/4), Switzerland. The excerpt consists of a stairway (left side), a ramp (middle), and a smoking area with recycling bins and ashtrays (right), as displayed in Fig. 5. Entrances/exits to the platform are located at the right side of the stairway and ramp, highlighted by red lines. Furthermore, the platform edges where trains will arrive are displayed by green lines. As this excerpt is only about 60 m long, we extended the geometry for the simulations by 50 m in both directions, such that pedestrian can move freely without being obstructed by the boundary. The original geometry contains multiple pillars in the top half of the platform, close to the ramp and between ramp and smoking area. We had to remove some of these pillars in our simulations, as their diameters were too small to be adequately handled by the library used to compute the visible area.

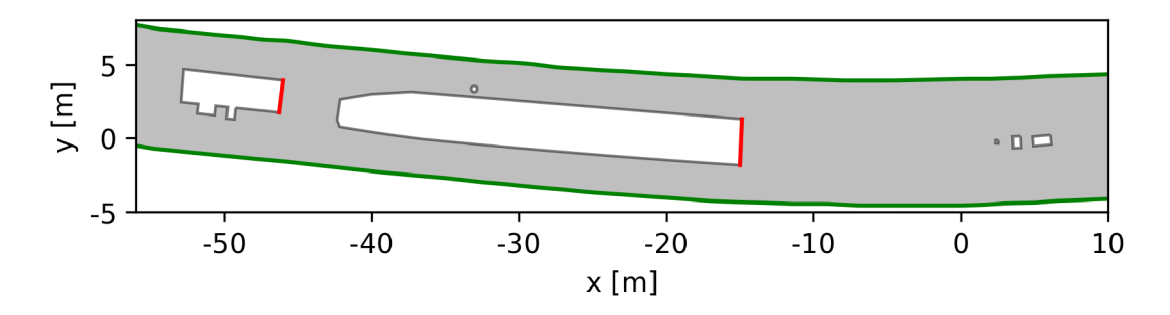


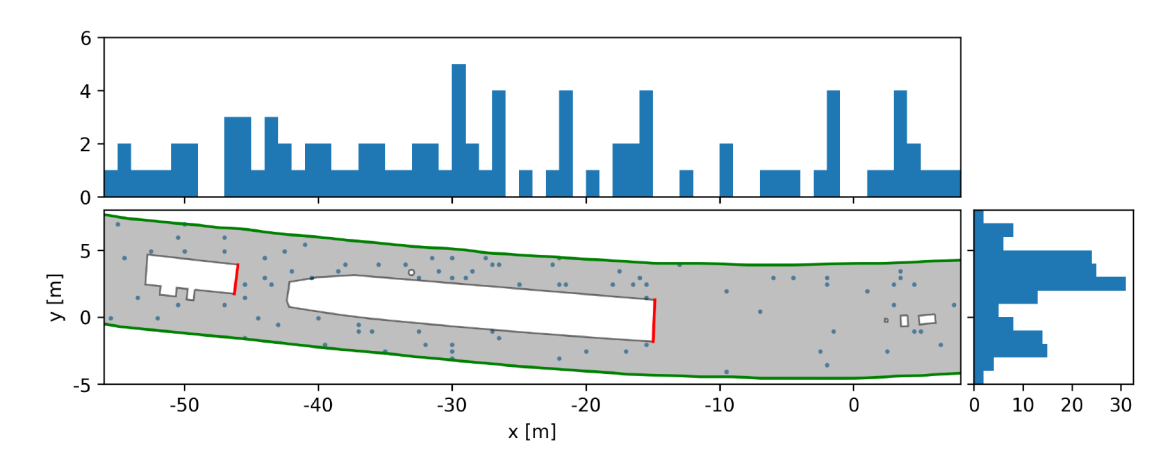
FIGURE 5: Excerpt of the platform in Bern, Switzerland used for the simulations. White areas mark obstacles as stairway (left), ramp (middle), and recycle bins and ash trays (right). Red lines indicate the entrances/exits of the platform, green lines are the platform edges.

For simulating different initial situations and waiting times, multiple simulations have been conducted varying different input parameters, as shown in Tab. 1. We decided for short time intervals between the trains, e.g., 3 min, 5 min, and 10 min to simulate peak traffic times. The maximum number of pedestrians in the simulations varies between 200, 300, and 500. The number of pedestrians initially distributed on the platform depends on the maximal number pedestrians in the simulation. In our simulations either 25% or 50% of the maximal number of pedestrians are already distributed on the platform. Other pedestrians enter the platform through one of the entrances with a constant flow. For pedestrians entering the platform, a goal, bottom, or top platform edge, based on a weighted random selection is chosen.

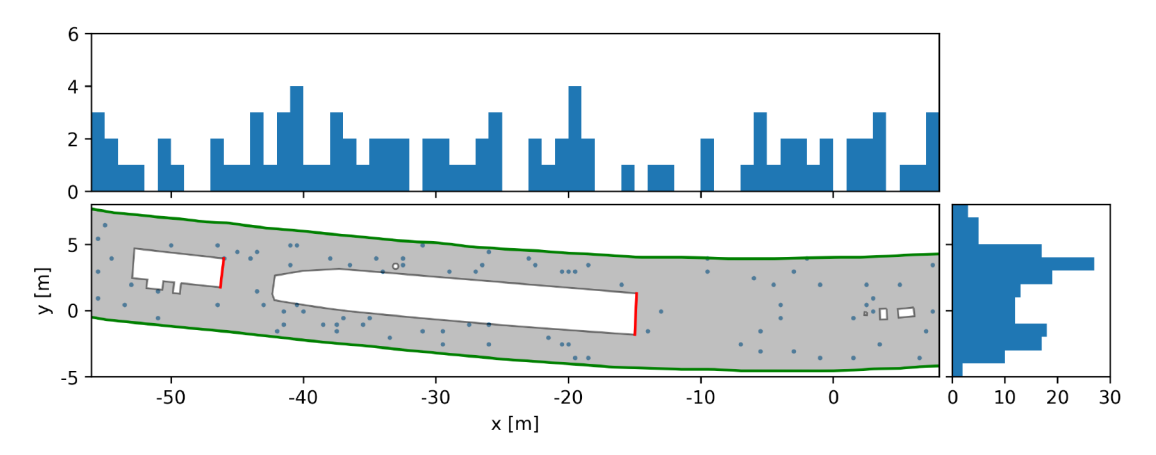
TABLE 1: Used initial situations for the simulation

time	max. agents	initial agents	prob. of ped. for bottom track
3 min, 5 min, 10 min	200, 300, 500	25%, 50%	0%, 25%, 50%, 75%

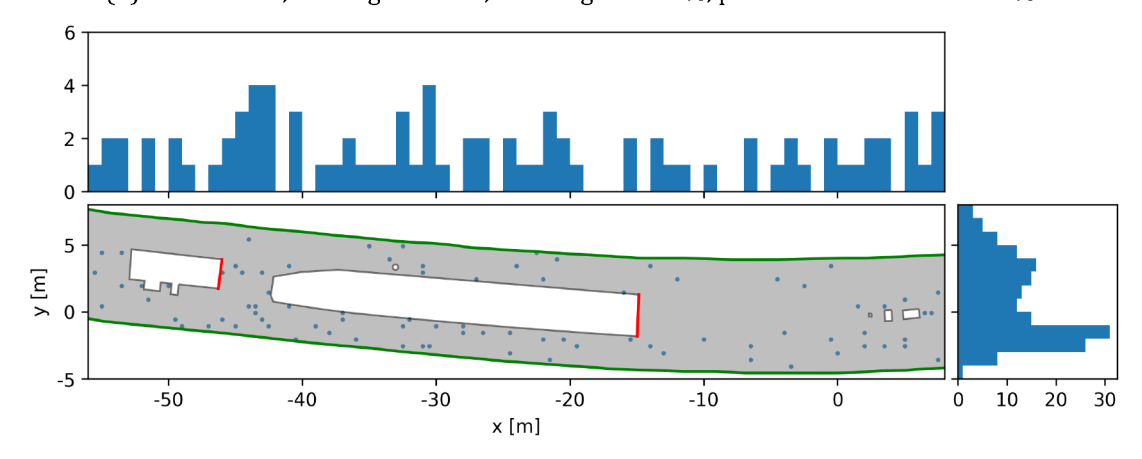
In several field observations [5, 15, 9, 13] on different train stations, the positions of entrances were emphasized as the the most important factor to the pedestrian longitudinal distributions on platforms. Clustering of pedestrians usually occurs close to platform entries and exits, leading to a non-uniform distribution and, in some cases, leaves parts of the platform empty, which are further away from entrances. The same behavior can be observed in our model. Fig. 6 shows the distribution of the waiting pedestrians at the end of the simulation. One can see that areas close to the entrances are preferred compared to further distanced positions. Furthermore, the preference of waiting positions close to platform infrastructure can be observed, as pedestrians' clustering close to the smoking area on the right side occurs. Also the preference of the platform side, where a train is expected to arrive, can be observed. In Fig. 6a most pedestrians wait for the train on the top platform edge, which is also reflected in the pedestrians distribution. As the number of pedestrians waiting for a train on the top decreases, the distribution shows a shift towards the bottom track Figs. 6b to 6c.



(A) Time: 3 min, max. agents: 300, initial agents: 50%, prob. for bottom track: 25%.



(B) Time: 3 min, max. agents: 300, initial agents: 50%, prob. for bottom track: 50%.



(c) Time: 3 min, max. agents: 300, initial agents: 50%, prob. for bottom track: 75%.

FIGURE 6: Comparison of pedestrian distributions on platform at the end of the simulation.

Küpper and Seyfried [10] introduced the measure occupation of space in their work, which allows to identify hot spots where passengers tend to wait for a train. For the measure the space is divided into regular cells. The usage of each cell is increased by one every time it is occupied by a passenger. The occupation of a cell is normalised with the number of frames. They analyzed the afternoon peak traffic times between 3:30 pm and 6:00 pm and computed the corresponding occupation of space, shown in Fig. 7a. We use the same method to compute the occupation of space, averaged over multiple simulations. The results are shown in Fig. 7b. The hot spots close to the walls of the stairway, the ramp and the smoking area can be observed. As we had to remove some of the pillars from the platform due to their size, some of the hot spots visible in [10] are not that distinct or are missing, e.g., in the area between ramp and smoking area. Since we conducted 200 simulations and computed the average over all, the hot spots are more spread compared to the sensor data, as here only roughly 20 trains arrive at the platform. Another difference is introduced as we only focus on boarding passengers waiting on the platform and neglect any alighting

passengers. These pedestrians will increase space occupation, especially in front of the platform's entrances/exits. Despite these differences between real-life scenarios and our simulations, our results show good agreement with the real platform's tracking data.

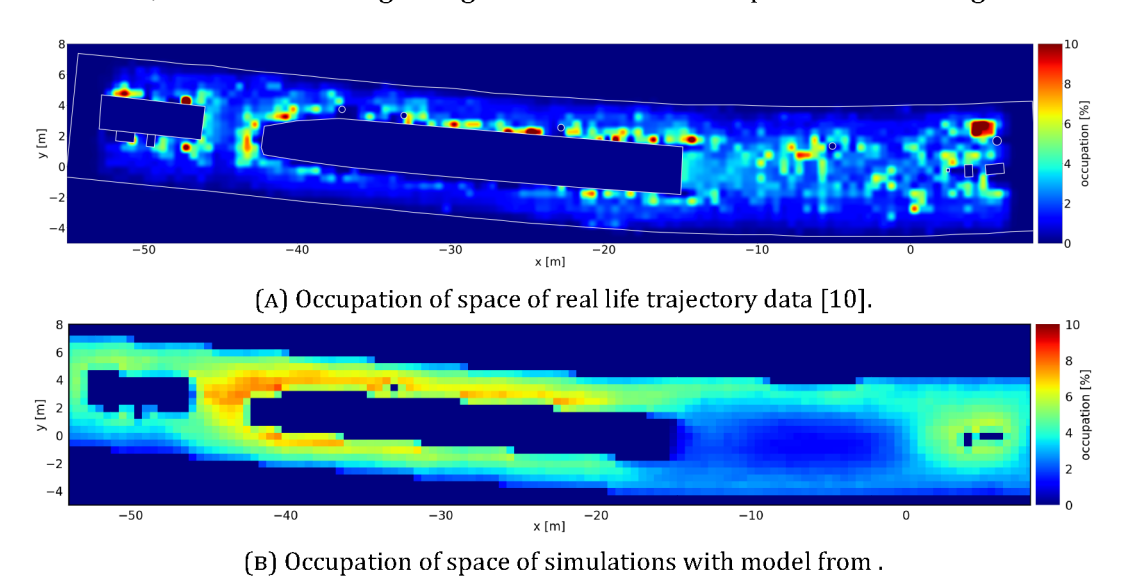


FIGURE 7: Comparison of the occupation of space from real-life tracking data and simulation of waiting pedestrians with the model from .

CONCLUSION & OUTLOOK

In this work, we developed a cellular automaton for modeling pedestrians' waiting behaviors at train stations. The model is based on potential fields derived from different influence factors found in experiments and field studies. Behaviors that could be observed in real-life tracking data and are reported in field observations, as the clustering close to entrances or close to platform infrastructure, can also be seen in the presented model. In particular, the occupation of space shows good agreement with the tracking data.

Additional factors, such as attraction, repulsion, or danger zones, can be easily added to the model to improve the model further. With extensive parameter studies, the influence of each potential field could be analyzed in more detail. These results could derive parameter sets for different types of travelers, e.g., commuters, tourists, for the simulation. One factor currently missing in the model is group behavior. Groups traveling together would also choose a waiting position suitable for the whole group. A possible solution for this is introducing an additional potential field that would highly reward proximity to the group.

As pedestrians may move to each direction in each time step, some unnatural behavior as walking in circles or walking back and forth can be observed. One possible solution may be to weigh the potential fields' probabilities depending on the movement from the previous step to penalize sharp turns. It is rather unlikely that a pedestrian comes to a halt for a longer time in the current model. This could be changed by rewarding staying at the current position, depending on the time spent in a particular cell.

ACKNOWLEDGMENT

This work has been performed within the research program "Optimizing the capacity of train stations in case of large-scale emergency evacuation events" (KapaKrit) funded by the German Federal Ministry of Education and Research-BMBF(grant numbers 13N14619 to 13N14621).

REFERENCES

- [1] Carsten Burstedde et al. "Simulation of pedestrian dynamics using a two-dimensional cellular automaton". In: *Physica A: Statistical Mechanics and its Applications* 295.3 (2001), pp. 507–525. ISSN: 0378-4371. DOI: https://doi.org/10.1016/S0378-4371(01)00141-8.
- [2] Mohcine Chraibi, Armin Seyfried, and Andreas Schadschneider. "Generalized centrifugal-force model for pedestrian dynamics". In: *Physical Review E* 82.4 (Oct. 2010). DOI: 10.1103/physreve.82.046111.
- [3] Maria Davidich et al. "Waiting zones for realistic modelling of pedestrian dynamics: A case study using two major German railway stations as examples". In: *Transportation Research Part C: Emerging Technologies* 37 (Dec. 2013), pp. 210–222. DOI: 10.1016/j.trc.2013.02.016.
- [4] Takahiro Ezaki et al. "Inflow Process of Pedestrians to a Confined Space". In: *Collective Dynamics* 1 (July 2016). DOI: 10.17815/cd.2016.4.
- [5] Wiktoria Heinz. *Passenger service times on trains*. Tech. rep. Stockholm: KTH Royal Institute of Technology, 2003.
- [6] Dirk Helbing and Péter Molnár. "Social force model for pedestrian dynamics". In: *Physical Review E* 51.5 (May 1995), pp. 4282–4286. DOI: 10.1103/physreve.51.4282.
- [7] Fredrik Johansson, Anders Peterson, and Andreas Tapani. "Waiting pedestrians in the social force model". In: *Physica A: Statistical Mechanics and its Applications* 419 (Feb. 2015), pp. 95–107. DOI: 10.1016/j.physa.2014.10.003.
- [8] Ansgar Kirchner and Andreas Schadschneider. "Simulation of evacuation processes using a bionics-inspired cellular automaton model for pedestrian dynamics". In: *Physica A: Statistical Mechanics and its Applications* 312.1 (Sept. 2002), pp. 260–276. ISSN: 03784371. DOI: 10.1016/S0378-4371(02)00857-9.
- [9] Nikola Krstanoski. "Modelling Passenger distribution on Metro Station Platform". In: *International Journal for Traffic and Transport Engineering* 4.4 (Dec. 2014), pp. 456–465. DOI: 10.7708/ijtte.2014.4(4).08.
- [10] Mira Küpper and Armin Seyfried. "Analysis of Space Usage on train station platforms based on trajectory data". In: *Sustainability* (to appear). ISSN: 2071-1050.

- [11] Xiaodong Liu et al. "Typical features of pedestrian spatial distribution in the inflow process". In: *Physics Letters A* 380.17 (Apr. 2016), pp. 1526–1534. DOI: 10.1016/j.physleta.2016.02.028.
- [12] James A Sethian. "A fast marching level set method for monotonically advancing fronts". In: *Proceedings of the National Academy of Sciences* 93.4 (1996), pp. 1591–1595.
- [13] D. Szplett and S. C. Wirasinghe. "An investigation of passenger interchange and train standing time at LRT stations: (i) Alighting, boarding and platform distribution of passengers". en. In: *Journal of Advanced Transportation* 18.1 (1984), pp. 1–12. ISSN: 2042-3195. DOI: 10.1002/atr.5670180102.
- [14] Antoine Tordeux, Mohcine Chraibi, and Armin Seyfried. "Collision-Free Speed Model for Pedestrian Dynamics". In: *Traffic and Granular Flow '15*. Ed. by Victor L. Knoop and Winnie Daamen. Springer International Publishing, 2016, pp. 225–232. DOI: 10. 1007/978-3-319-33482-0_29.
- [15] Paul B.L. Wiggenraad. *Boarding and Alighting Time in Dutch Rail Stations*. Tech. rep. Delft: TRAIL Research School, 2001.
- [16] Xiaoxia Yang et al. "A Cost Function Approach to the Prediction of Passenger Distribution at the Subway Platform". In: *Journal of Advanced Transportation* 2018 (Oct. 2018), pp. 1–15. DOI: 10.1155/2018/5031940.